

Article

# Piezoelectric Silicon Micropump for Drug Delivery Applications

Agnes Bußmann <sup>1,2,\*</sup> , Henry Leistner <sup>1,3</sup> , Doris Zhou <sup>1</sup> , Martin Wackerle <sup>1</sup>, Yücel Congar <sup>1</sup>, Martin Richter <sup>1</sup> and Jürgen Hubbuch <sup>2</sup>

<sup>1</sup> Fraunhofer EMFT Research Institution for Microsystems and Solid State Technologies, 80686 Munich, Germany; henry.leistner@emft.fraunhofer.de (H.L.); doris.zhou@emft.fraunhofer.de (D.Z.); martin.wackerle@emft.fraunhofer.de (M.W.); yuecel.congar@emft.fraunhofer.de (Y.C.); martin.richter@emft.fraunhofer.de (M.R.)

<sup>2</sup> Institute of Engineering in Life Sciences, Section IV: Biomolecular Separation Engineering, Karlsruhe Institute of Technology (KIT), 76131 Karlsruhe, Germany; juergen.hubbuch@kit.edu

<sup>3</sup> Department of Electrical and Computer Engineering, Technical University of Munich (TUM), 80333 Munich, Germany

\* Correspondence: agnes.bussmann@emft.fraunhofer.de; Tel.: +49-89-54759-416

**Abstract:** Subcutaneous injection is crucial for the treatment of many diseases. Especially for regular or continuous injections, automated dosing is beneficial. However, existing devices are large, uncomfortable, visible under clothing, or interfere with physical activity. Thus, the development of small, energy efficient and reliable patch pumps or implantable systems is necessary and research on microelectromechanical system (MEMS) based drug delivery devices has gained increasing interest. However, the requirements of medical applications are challenging and especially the dosing precision and reliability of MEMS pumps are not yet sufficiently evaluated. To enable further miniaturization, we propose a precise  $5 \times 5 \text{ mm}^2$  silicon micropump. Detailed experimental evaluation of ten pumps proves a backpressure capability with air of  $12.5 \pm 0.8 \text{ kPa}$ , which indicates the ability to transport bubbles. The maximal water flow rate is  $74 \pm 6 \mu\text{L}/\text{min}$  and the pumps' average blocking pressure is  $51 \text{ kPa}$ . The evaluation of the dosing precision for bolus deliveries with water and insulin shows a high repeatability of dosed package volumes. The pumps show a mean standard deviation of only  $0.02 \text{ mg}$  for  $0.5 \text{ mg}$  packages, and therefore, stay below the generally accepted 5% deviation, even for this extremely small amount. The high precision enables the combination with higher concentrated medication and is the foundation for the development of an extremely miniaturized patch pump.

**Keywords:** micropump; piezoelectric diaphragm pump; drug delivery; microdosing; patch pump; insulin delivery



**Citation:** Bußmann, A.; Leistner, H.; Zhou, D.; Wackerle, M.; Congar, Y.; Richter, M.; Hubbuch, J. Piezoelectric Silicon Micropump for Drug Delivery Applications. *Appl. Sci.* **2021**, *11*, 8008. <https://doi.org/10.3390/app11178008>

Academic Editor: Eric Chappel

Received: 30 July 2021

Accepted: 25 August 2021

Published: 30 August 2021

**Publisher's Note:** MDPI stays neutral with regard to jurisdictional claims in published maps and institutional affiliations.



**Copyright:** © 2021 by the authors. Licensee MDPI, Basel, Switzerland. This article is an open access article distributed under the terms and conditions of the Creative Commons Attribution (CC BY) license (<https://creativecommons.org/licenses/by/4.0/>).

## 1. Introduction

Medical care relies strongly on pharmaceuticals to treat diseases. Intravenous or subcutaneous injections are an easy and very common way of administration. However, manual injections can be uncomfortable, require regular attention, and do not offer the possibility of continuous dosing. Automated delivery can circumvent these disadvantages.

One well-known drug dosing application is the treatment of diabetes. The strict management of the blood glucose level is crucial for the patients well-being [1]. It is known that continuous subcutaneous insulin delivery with a pump system improves patient's care significantly compared to multiple daily injections [2–4]. Currently, two pump types for subcutaneous drug delivery are available: durable pumps in combination with an infusion set, and patch pumps. The latter reduce the need for regular disconnection, for instance when practicing sports or showering, and therefore enable a constant insulin supply. Moreover, the elimination of tubing leads to more comfortable and less visible use and therefore improves the patient's compliance. Consequently, patch pumps show to ameliorate the therapeutic success [5,6]. Continuous drug delivery to specific tissues also

leads to a better therapeutic result with limited side effects for specific cancer treatments and studies show that a delivery adapted to the circadian rhythm is beneficial [7,8].

Even though research pushes towards automated, small dosing units for patch applications or implantation, there is still improvement necessary [9]: existing patch pumps for insulin delivery are large enough to be visible under clothing. Furthermore, the accuracy of currently available pumps is lower compared to durable pumps [10–13]. The improvement of the dosing accuracy as well as further miniaturization is therefore desirable.

The drug delivery application demands for well-adapted properties under challenging conditions [9]. The device needs to be utmost reliable with high dosing accuracy and dosing stability, even against backpressure. In addition to demanding fluidic requirements, patch pumps need to be cost-efficient, since they are often at least partly disposable and need to compete with the cost of conventional therapy.

Further miniaturization of delivery systems is possible based on micropumps that enable small and lightweight systems for energy efficient delivery. Since the production is mostly based on standard, large scale processes, e.g., MEMS processes, costs are low if production numbers are sufficiently high. However, the use of micropumps implies new challenges. For instance, the transport of air bubbles that is usually unproblematic for macroscopic actuators, can lead to the failure of a micro diaphragm pump, since air is compressible and acts as a fluidic capacitance in the chamber of the displacement pump [14]. Additionally, surface tension becomes extremely relevant and the microfluidic actuator needs to be capable of moving the liquid meniscus through the system while overcoming resulting capillary forces [15–17]. Bubble tolerance of diaphragm pumps can be achieved with adapted designs towards a large compression ratio, the ratio between displaced volume and dead volume, that enables to overcome high air backpressure [14].

To enable the use of micropumps for drug delivery application, a sufficient dosing accuracy has to be guaranteed. However, up to date, micropumps presented in research are not tested extensively with respect to their dosing precision and reliability [9]. The only extensively tested, MEMS based patch pump system is the Jewel Pump developed by DeBiotech. The integration of a double limiter concept, several pressure sensors and the pre-tension of the passive flap valves enable stable dosing even at varying temperature, inlet and outlet pressure, or medium's viscosity as well as a quick error detection [18–20]. Borot et al. [13] confirm a high dosing accuracy compared to other insulin pump systems, and an exceptionally fast error detection.

To further evaluate the usability of micropump based delivery systems, a detailed experimental characterisation of the fluidic properties, as well as the dosing precision and robustness of the fluidic actuator are necessary. However, the little volume of dosed packages and the small measured flow rates make an experimental evaluation extremely challenging.

The norm IEC 60601-2-24 [21] regulates the assessment of dosing accuracy for drug dosing devices, also including patch pumps. Unfortunately, the proposed gravimetric measurement is not described in detail and data are to be presented in a trumpet curve, which is often criticised by the scientific community [22]. In addition, the norm allows for a run-in period of up to one day that does not reflect the clinical application where accurate dosing is required at all times [22,23]. Hence, several improvements to the experimental assessment of dosing accuracy are proposed to evaluate insulin delivery systems: It is common to depict the average deviation of the dosed volume within a given observation time, or the accuracy of single doses [10–13,23–25]. While optical flow detection that evaluates the volume in an accurate capillary is also used [25], most studies rely on gravimetric measurements [11,13,23]. It is necessary to minimize the influence of evaporation and condensation, both to cover the surface of the reservoir with oil [11,13,23] as well as an evaporation trap are adequate methods [26]. Furthermore, hydrostatic pressure can influence the measurement, which is why the inlet and outlet reservoir should be levelled [23]. Even if drift is prevented with all means, drift correction is indispensable for accurate data analysis.

In this work, we use a gravimetric measurement based on the introduced studies to evaluate the dosing precision of our piezoelectric micropump. The  $5 \times 5 \times 0.6 \text{ mm}^3$  small pump is specifically designed for the requirements of drug delivery, including fluidic performance such as flow and pressure capability, as well as the ability to transport bubbles. The precision of package dosing is investigated with water and insulin solution. Therewith, we evaluate the reproducibility of bolus dosing and investigate additional challenges caused by the change of the transported medium. This preliminary study is designed to investigate a general feasibility and reveal necessary improvements. The accuracy of an integrated pump in a closed-loop controlled dosing unit is the subject of subsequent studies.

## 2. Materials and Methods

All investigations in this work are conducted with Fraunhofer EMFT's  $5 \times 5 \times 0.6 \text{ mm}^3$  micropumps [27]. Compared to former versions of the pump, the chamber height is increased to  $20 \mu\text{m}$  and the valve seat circumference as well as flap area are increased. Therewith, the fluidic resistance is reduced, which enables higher flow rates and the transport of higher viscous fluids.

A set of ten pumps is used to establish statistical significance. All wetted surfaces are composed of silicon and respective native oxides. The pump consists of two valve layers and the actuator diaphragm with the glued on piezoelectric disc actuator (Figure 1). Fluid transport bases on the indirect piezoelectric effect: an alternating high voltage signal causes the piezoelectric ceramic to expand and contract and thus induces an oscillating upwards and downwards movement of the diaphragm. The resulting expansion and contraction of the pump chamber leads, in combination with the passive flap valves, to a directed fluid flow.

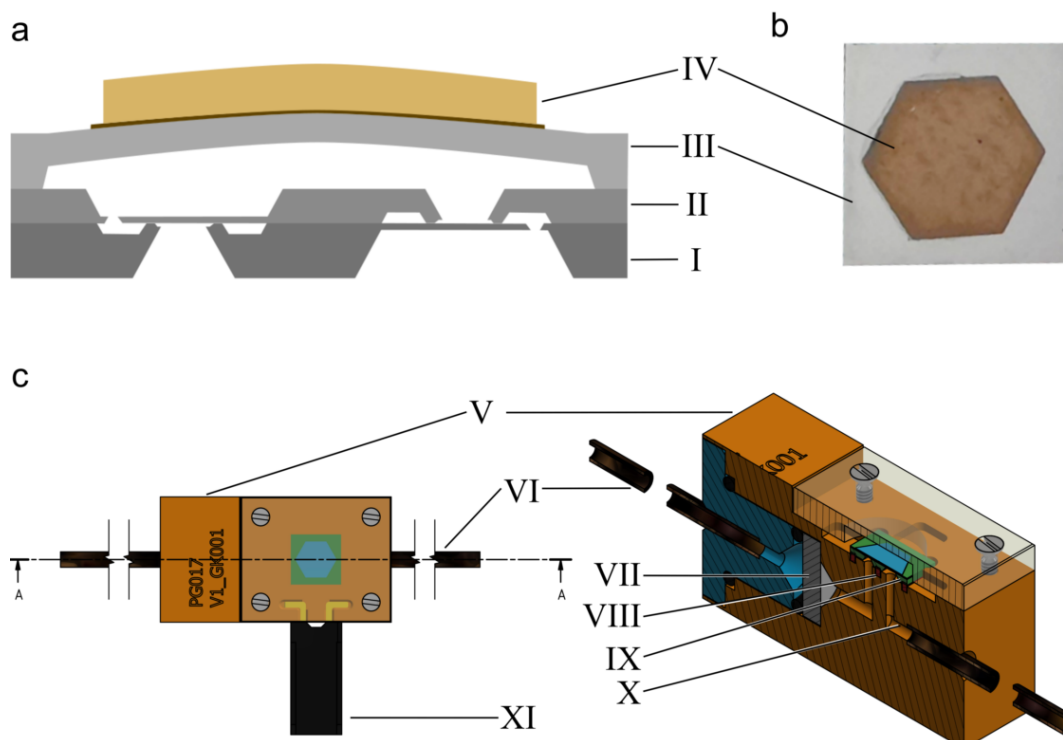


**Figure 1.** Schematic cross-section (a) of a  $5 \times 5 \times 0.6 \text{ mm}^3$  silicon micropump (b) with a 4.5 mm pump chamber diameter. The three grey layers represent the silicon pump body with the lower valve unit (I), the upper valve unit (II), and the actuator diaphragm (III) with the glued on piezoceramic (IV). For the fluidic characterization, the pumps (IX) are mounted into a test housing (c) that consists of a polyether ether ketone body (V) with drilled fluidic paths (X), inlet and outlet capillaries (VI), a stainless-steel filter (VII), and a soft sealing (VIII).

The pumps are manufactured based on standard silicon processes (Figure 2). For the valve structure, two n-doped silicon (100) wafers are covered with a silicon dioxide/silicon nitride hard mask that is subsequently structured by a lithography and dry etching process step (1). After the first KOH wet etching (2), one wafer is flipped and the wafers are bonded to form the valve unit. After oxidation and bonding the valve wafer stack is finalized with a grind and polishing step (3). A third silicon wafer (100) with a pre-etched micropump chamber is bonded on top of the valve wafer stack (4) and a grind and a spin etching process step finalize the actuator diaphragm of the micropump (5). The piezoelectric disc actuator is glued on the actuator diaphragm using a two-component epoxy adhesive (6). Table A1 (Appendix A) gives an overview of the used material.

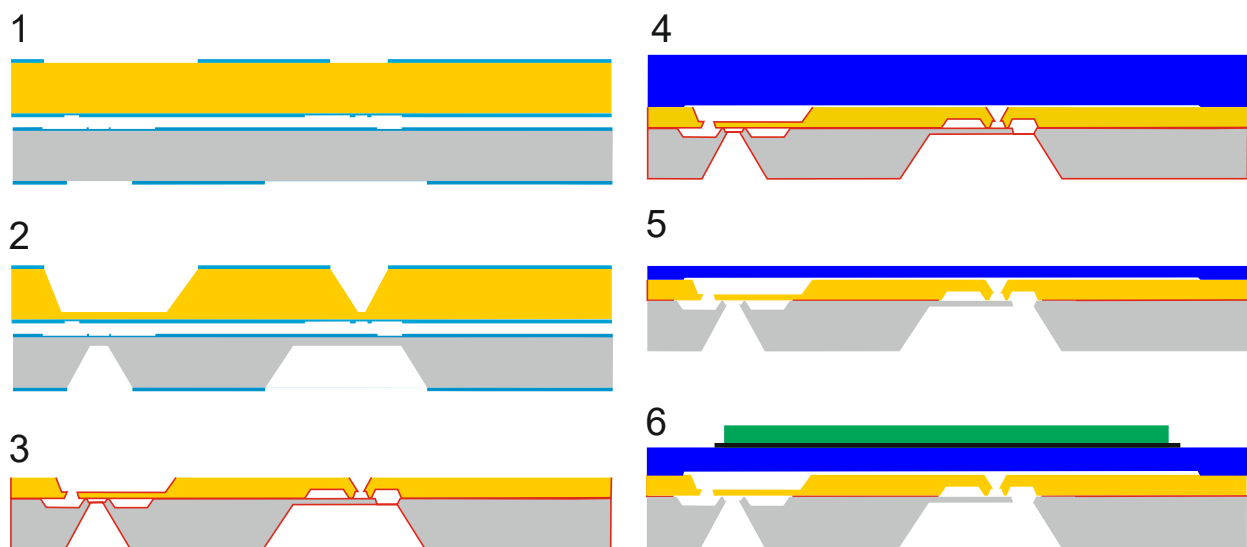


**Figure 2.** Schematic depiction of the process steps to manufacture the silicon micro diaphragm pump starting with the application of a structured hard mask (1) and subsequent KOH wet etching (2) of the two valve wafers. After oxidation, bonding, and a grind step (3) the actuator diaphragm with a pre-etched micropump chamber is bonded on top of the valve wafer stack (4). The diaphragm is finalized by a grind and spin etching process step (5) and the piezoelectric disc actuator is glued on the actuator diaphragm (6).

Bubble tolerance of the pumps is achieved with a specific adhesion process for the piezoelectric actuator [28]. During the curing phase, we apply an electric field that puts the ceramic in its contracted state. Once the glue is hardened, the voltage is disconnected and the ceramic expands and therewith bulges up the pump chamber. Due to this mounting technique, the compression ratio (ratio of displaced volume to dead volume in the chamber), is high, which is a condition for a high backpressure capability with compressive fluids as well as robust bubble tolerance. The compression ratio of the silicon micropump is estimated from its design: due to exact silicon manufacturing techniques, the volume of the pump chamber can be calculated easily. The stroke volume is determined analytically and confirmed during the fluidic characterisation of the pumps. Based on the dead volume and the single stroke volume, we calculate the compression ratio.

The power consumption of the pump itself can be estimated considering the piezoelectric actuator as ideal capacitor. The used disc actuators have a capacitance of 2.45 nF. An actuation optimized for liquid transport (120 V<sub>pp</sub> and 65 Hz) results in approximately 1.2 mW. To achieve maximal air flow, a higher voltage amplitude and a high frequency (150 V<sub>pp</sub> and 1.6 kHz) are necessary, which requires approximately 440 mW, though an operation with a lower frequency is possible to limit the power consumption.

For the large-scale production of the pump, we intend both, the entire manufacturing including piezo mounting, and the fluidic test of the pump to be realized on wafer-level. To this end, we developed a wafer-level tester that allows to reduce costs significantly [29]. Assuming 200 wafer starts per week with an 8-inch process resulting in approximately

10 million pumps/year, we estimate 0.8 €/pump including front end, back end and test costs. This price bases on a yield of 90% and does not comprise any margin, or additional costs for medical devices and regulatory affairs.

The ten pumps examined in this work are mounted into polyether ether ketone (PEEK) housings with glued in PEEK capillaries for fluidic connection (Figure 1). The pump chip is clamped onto a fluorine rubber sealing. At its inlet, the housing holds a stainless-steel filter unit with a pore size of 5  $\mu\text{m}$ . The silicon pump chips remain in the housing for all conducted experiments.

### 2.1. Basic Characterization

The basic characterization of the micropumps includes optical stroke measurement, air flow characterization, and water flow characterization.

The optical stroke measurement evaluates the deflection of the actuator diaphragm due to a quasi-static voltage signal. The actuator position is detected with a white light profilometer (MicroProf 100—CWL, FRT GmbH) including an optical sensor with a range of 300  $\mu\text{m}$  and resolution of 100 nm. The quasi-static voltage signal in a range from  $-50$  to 120 V is applied with a piezo amplifier (SVR 500—3, piezosystem jena GmbH). This voltage expands beyond the normal actuation voltage to enable the detection of mechanical contact between the actuator diaphragm and the chamber bottom shortly outside of the normal actuation range.

Part of the characterization with air are the maximal achievable flow rate as well as pressure capability of the actuated micropump. We detect the air mass flow with an EL-Flow prestige ( $\pm 0.5\%$  accuracy, Bronkhorst) at the inlet of the fluid path. The backpressure is measured with the pressure sensor 26PCCFA6D ( $\pm 1$  kPa accuracy, Honeywell) at the outlet of the closed fluid path. The alternating voltage signal of  $-30$  to 90 V is applied with an Agilent 33120A frequency generator and amplified with a piezo amplifier. To determine leakage rates, a controlled pressure (CPC3000, WIKA Mensor) is applied to the turned off pump's outlet and the resulting flow is detected (EL-Flow mass flow meter) at the pump's inlet.

The flow characterization with water includes the achieved mass flow at different backpressures from 0.2 to 40 kPa. It is performed with a purpose-built fluidic setup: The reservoir, sensors and pump are connected with steel capillaries. The inner diameter of the capillaries is sufficiently large and therefore has a neglectable influence on the detected flow rate. A worst-case estimation based on the Hagen–Poiseuille equation results in a pressure loss of only 0.04%. Pressure is applied as a nitrogen head-pressure over the outlet reservoir with a pressure generator (Mensor CPC3000) and verified in the fluid path 30 cm away from the pump with a Transducer WU-15 (WIKA). The water mass flow is determined with a Liqui-Flow from Bronkhorst ( $\pm 1\%$  accuracy). Amplification of the 15 Hz rectangular waveform with sinusoidal flanks (approximately 130 Hz) is achieved with an SVR 500/3 amplifier from Piezomechanik GmbH.

### 2.2. Bolus Characterization

The dosing precision of our silicon micropumps is determined with deionized water as well as insulin solution. A microgravimetric measuring method based on IEC 60601-2-24 and the setup proposed by Freckmann et al. [24] is used to determine the water bolus precision. A schematic of the experimental installation is shown in Figure 3. Experimental characterization of the package dosing with water is conducted with nine pumps. Purified DI water is pumped from an input reservoir to an output reservoir which is placed on the Sartorius 225S scale (0.025 mg reproducibility). The pump is installed outside the scale's measurement chamber in a casing. PEEK tubes (IDEX Health&Science 1538) are connected to the inlet and outlet tubes of the pump's casing and inserted into the water in the inlet and outlet reservoir. The used capillaries have an inner diameter of 1 mm. The distance to the inlet is approximately 20 cm and the capillary length to the outlet approximately 40 cm. Both input and output reservoir are filled with water such that the surfaces are leveled

to avoid effects of hydrostatic pressure. A 2 mm thick layer of oil (thermo scientific E33 (12017/00043)) is dispensed onto the water in the output reservoir to prevent evaporation.

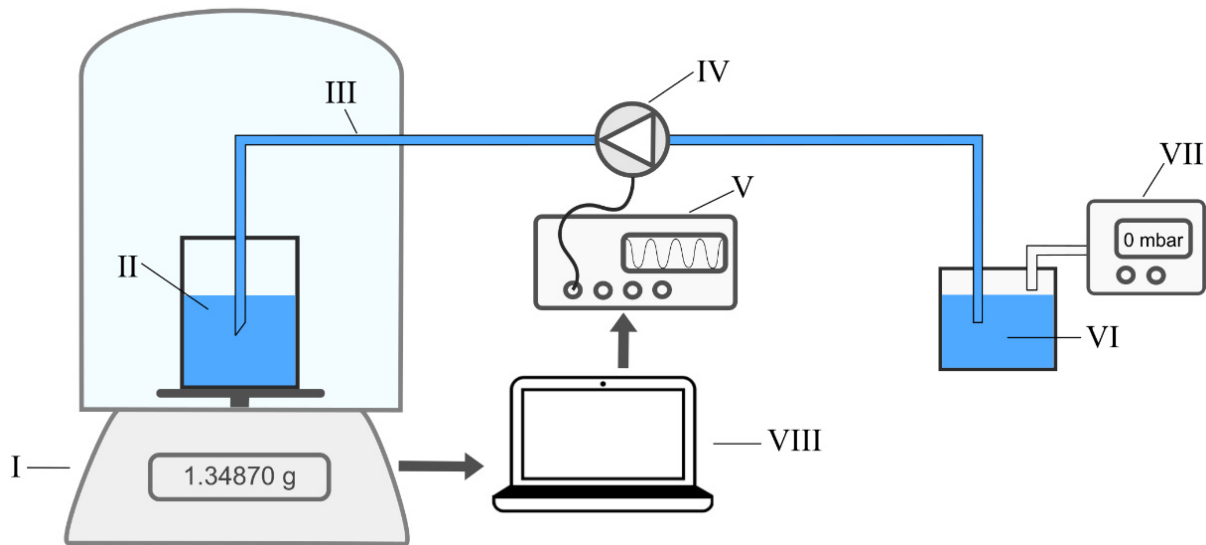


**Figure 3.** Experimental setup for the gravimetric measurement of package dosing. The pump (IV) transports liquid through PEEK capillaries (III) from the inlet reservoir (VI) toward the outlet reservoir (II) that is placed on a balance (I). The pump is actuated with a signal generator and amplifier (V) and controlled with a laptop (VIII) that collects the recorded weight data. For priming, the inlet is connected with a pressure controller (VII).

The used silicon pumps are self-priming. However, to rapidly prime the dead volume of the setup, the system is passively primed. After the pump is connected we apply a positive pressure of 200 mbar to the inlet reservoir (Mensor CPC4000 pressure controller) until no further air emerges from the outlet capillary. This priming procedure enables accurate measurements, since remaining bubbles in the fluid path and especially fluidic connectors are flushed out of the system. A Keysight 33500B waveform generator and a Piezomechanik SVR 500–1 amplifier are used to generate a rectangular waveform with sinusoidal flanks (100 Hz) with a voltage of  $-30/+90$  V and a frequency to 65 Hz to operate the micropump.

The measurements are conducted for three bolus sizes of approximately 0.5025 mg, 5.025 mg, and 50.25 mg. For U100 insulin solution, these packages sizes correspond to 0.05 international units (U), 0.5 U, and 5 U of insulin. In this experiment, the pumps are not closed-loop controlled and the number of strokes needed for a given bolus size is calculated with the average stroke volume of this pump type. Variation of the pumps due to manufacturing tolerances can cause the average bolus volume to deviate. We therefore do not aim to evaluate dosing accuracy, but rather the repeatability of package dosing, meaning the dosing precision. A calibration on each individual pump's stroke volume or a closed-loop control can later be implemented to achieve sufficient accuracy. For each bolus size and individual pump, we dose forty volume packages by repeating a sequence of four dosages (active pump) and one subsequent reference measurement without dosing (inactive pump) for ten times. During the reference measurement, the pump is not actuated, no fluid is transported, and the resulting dosed volume after drift correction should be zero. Hence, the reference measurement without pump actuation allows us to detect errors in the experimental setup. Based on the water characteristics for a pump frequency of 65 Hz, one actuator stroke delivers in average 62  $\mu\text{g}$  of water. Thus, for the different bolus sizes, the required number of single strokes is computed to 8, 81, and 815 with a corresponding active time per dosage of 0.12 s, 1.25 s, and 12.54 s. The data are drift compensated based on approximately 33 s drift measurement conducted before each dosed bolus.

Insulin dosage is evaluated with U100 of NovoRapid<sup>®</sup> (trivial name: insulin aspart) from the company Novo Nordisk, where one milliliter of the solution contains 100 interna-

tional units (3.5 mg) of insulin. The experimental setup and procedure remain the same as was used for the characterization of the dosing precision with water. The only adaptation is the inlet reservoir, where we used a smaller jar to account for the limited sample volume. Due to a limitation of the insulin volume, the dosage of large packages was only possible for nine out of ten pumps.

### 3. Results and Discussion

Drug delivery applications require very specific characteristics, which makes a detailed experimental analysis indispensable. The results presented in this work include the evaluation of ten individual micropumps of the same batch regarding the silicon micromachining (frontend), piezo mounting (backend) and assembly.

#### 3.1. Standard Characterization

The characteristics and fluidic performance of the ten micropumps used for the evaluation of the dosing precision are summarized in Table 1.

**Table 1.** Average mechanical and fluidic characteristics of the ten evaluated piezoelectric silicon micropumps at a given actuation signal (amplitude; frequency).

Fluid	Characteristics	Actuation	Mean Value
-	Actuator stroke	−20/+100 V; quasi-static	15.0 ± 1.1 μm
Air	Flow rate	−50/100 V; 1.6 kHz −30/90 V; 65 Hz	6.5 ± 0.5 min 0.26 ± 0.07 min
Air	Backpressure	−30/90 V; 65 Hz	14.3 ± 0.3 kPa <sup>1</sup>
DI water	Flow rate at 0 kPa	−30/90 V; 15 Hz	0.074 ± 0.006 min
DI water	Blocking pressure	−30/90 V; 15 Hz	51.2 ± 0.9 kPa <sup>1</sup>

<sup>1</sup> The air backpressure and water blocking pressure are calculated from a linear fit of the backpressure measurement as depicted in Figure 4.

The first indication for the functionality of a diaphragm pump is the achievable actuator stroke, since it directly determines the volume displaced within one pump cycle and, hence, achievable flow rates. Furthermore, the optical actuator stroke measurement allows to detect a touchdown, i.e., the mechanical blocking of further movement when the diaphragm reaches the chamber bottom. It causes a characteristic kink in the displacement curve and limits the stroke volume. None of the tested pumps shows a touchdown. The average stroke ( $\Delta z$ ) of all ten microactuators achieved with −20 to 100 V quasi-static actuation is  $\Delta z = 15.0 \mu\text{m} \pm 1.1 \mu\text{m}$  leading to an approximate stroke volume ( $\Delta V = \pi \cdot R^2 / 3 \cdot \Delta z$ ) of  $\Delta V = 79 \text{ nL}$ . This volume corresponds well to the characterization of similar pumps by Leistner et al. [27].

All pumps are characterized regarding their air transport, e.g., backpressure capability as well as frequency dependent air flow rate. The air flow achieved with an actuation frequency of 65 Hz and a peak to peak voltage of 120 V, which is the signal used for later bolus dosing, is  $0.26 \text{ mL/min} \pm 0.07 \text{ mL/min}$ . With an actuation optimized for air transport (−50/100 V; 1.6 kHz), the pumps achieve higher flow rates of  $6.5 \text{ mL/min} \pm 0.5 \text{ mL/min}$ .

The pressure capability when transporting air depends strongly on the compression ratio, which is approximately 0.15 for the  $5 \times 5$  silicon pump and is sufficient for gas transport [14,30]. Sufficient backpressure capability with air is a condition for bubble tolerance and therefore evaluated with the same actuation signal used for fluid transport, even though this actuation is not optimized for air transport. From a linear fit of the pressure dependent mean air flow of all samples we calculate a backpressure capability of  $14.3 \text{ kPa} \pm 0.3 \text{ kPa}$  (Figure 4).

The water flow rate with and without applied backpressure is analyzed for all pumps (Figure 4). Without additional backpressure, the mean water flow rate of the ten pumps is  $Q_{\text{water},0 \text{ kPa}} = 74 \mu\text{L}/\text{min} \pm 6 \mu\text{L}/\text{min}$ . With U100 insulin, this allows to deliver a bolus of 10 U in approximately 90 s and puts our micropump in the same range of delivery speed as currently available delivery systems [24].

A linear regression of the water flow rate at increasing backpressures allows to determine the blocking pressure, where the flow reaches zero. At 40 kPa the average achieved flow rate is  $Q_{\text{water},40 \text{ kPa}} = 16 \mu\text{L}/\text{min} \pm 7 \mu\text{L}/\text{min}$  and the linear regression shows an extrapolated blocking pressure of  $p_{\text{block}} = 51.2 \text{ kPa} \pm 0.9 \text{ kPa}$ . These results are in good agreement with previous research [27]. The high achievable pressure is necessary to overcome counterforces in a delivery system. While the pressure of the tissue as well as the fluidic backpressure of the channels are low for reasonable flow rates, clogging of the injection site might cause a high backpressure that the pump needs to overcome.

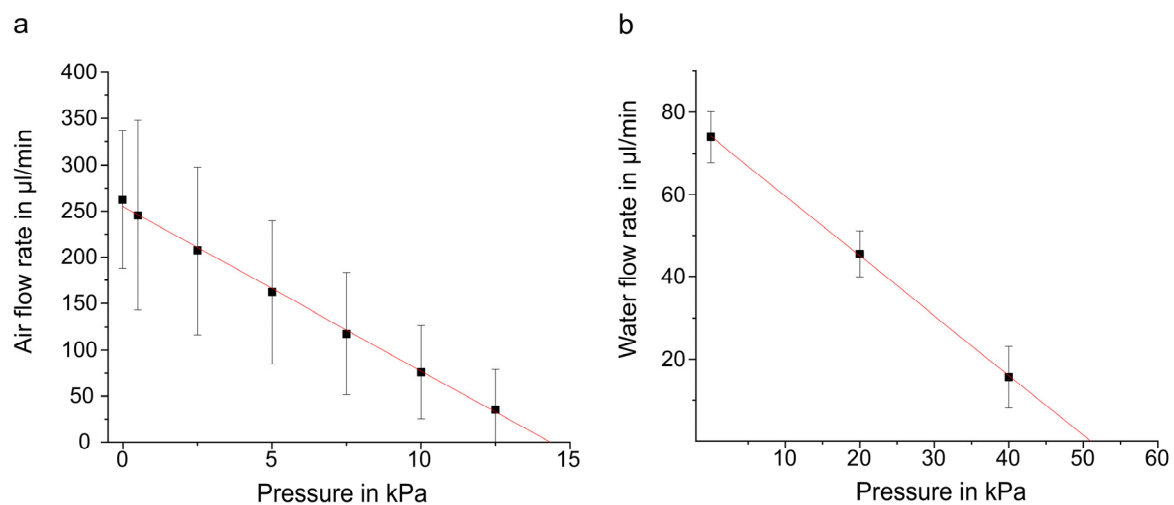


**Figure 4.** Flow characterization of the ten micropump samples. (a) Average air flow rate of the ten pumps at varying backpressure. The pumps are actuated with  $-30/90 \text{ V}$  and  $65 \text{ Hz}$ . The extrapolated achievable backpressure is  $14.3 \text{ kPa}$ . The error bars depict the standard deviation. (b) Average water flow rate of the ten pumps at varying backpressure. The pumps are actuated with  $-30/90 \text{ V}$  and  $15 \text{ Hz}$  rectangular waveform with sinusoidal flanks (approximately  $130 \text{ Hz}$ ). The extrapolated blocking pressure is  $51 \text{ kPa}$ . The error bars depict the standard deviation.

### 3.2. Bolus Precision Investigation

The repeatable precise dosing of small volume packages is indispensable for bolus drug delivery. In this work, we aim to evaluate the repeatability of package dosing of our  $5 \times 5 \text{ mm}^2$  micropump without the influence of a control unit. Thus, we test in an experimental setup that is not closed-loop controlled. We dose a package size that is defined by the number of single strokes performed and aims at an approximate quantity. However, small variations between the pumps due to manufacturing tolerances cause the average package size to differ slightly for the pumps. This deviation can later be prevented based on individual calibration and closed-loop control. However, a precondition for a well working controlled dosing unit is a high reproducibility of dosed individual volume packages. We, therefore, present a detailed investigation of our pump's dosing precision.

In preliminary experiments, we evaluate the package dosing with water. Figure 5 shows the precision of the tested pumps when dosing small, medium and large packages with approximately  $0.5 \text{ mg}$ ,  $5 \text{ mg}$ , and  $50 \text{ mg}$ , respectively. These packages are the equivalent mass of insulin solution needed to deliver  $0.05 \text{ U}$ ,  $0.5 \text{ U}$  and  $5 \text{ U}$  of insulin.

It is clearly visible that the dosage of extremely small packages is more challenging. The sample to sample variation between the forty individually dosed  $0.5 \text{ mg}$  packages is higher than for larger packages. However, the standard deviation also varies for the pumps and ranges from  $2.5\%$  to  $14.9\%$ . Five out of nine pumps show high dosing precision

even for small packages with a standard deviation of less than 3% and two pumps,  $\mu P_{03}$  and  $\mu P_{06}$ , show approximately 5% deviation, which is generally considered acceptable by pump manufacturers [23]. Only two pumps  $\mu P_{02}$  and  $\mu P_{05}$  dose the forty volume packages with a standard deviation of over 10%.

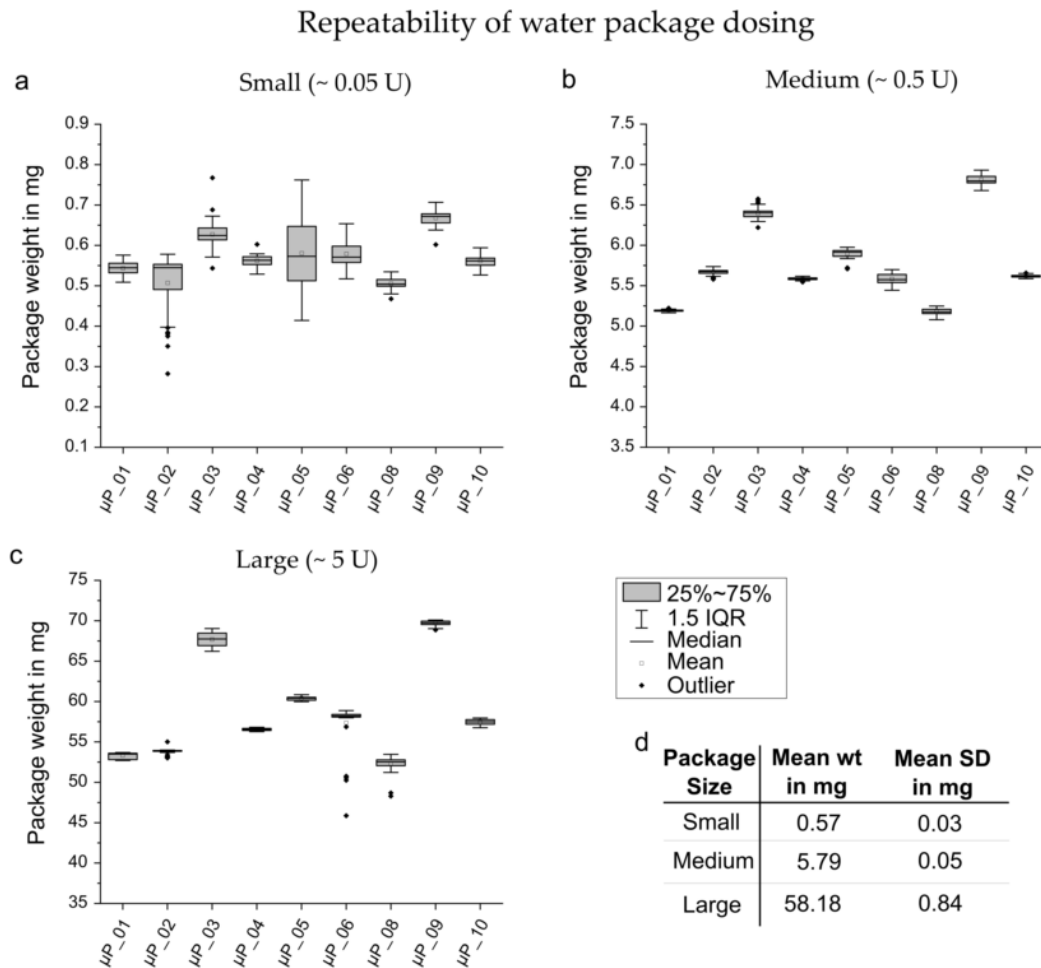


**Figure 5.** Repeatability of package dosing for each individual micropump ( $\mu P_{01}$  to  $\mu P_{10}$ ) with water for small (a), medium (b) and large (c) packages of approximately 0.5 mg, 5 mg and 50 mg, respectively. The overview (d) of the mean dosed weight and the mean standard deviation of all tested pumps shows an overall high dosing precision.

For larger packages, such as 5 mg and 50 mg the standard deviation tends to be smaller. For 5 mg packages it ranges from 0.2% to 1.8% with only one outlier,  $\mu P_{06}$ , with a standard deviation of 4.8%. This higher deviation is likely caused by air in the fluid path, since four consecutive out of forty packages deviate. This is likely the case if a bubble passes the pump and needs some strokes to be ejected before efficient fluid transport continues. The air can be entrapped in connectors, capillaries, or the edges of the test housing. Therefore, a geometric adaptation of the fluid path, e.g., reducing sharp edges, can facilitate priming and minimize the occurrence of bubbles that reduce the dosing precision. Such design recommendations also hold for fluid reservoirs and paths in the drug delivery application, since bubbles can also occur during drug dosing. Since it is impossible to reliably prevent bubbles at all times, the higher deviation detected for one sample is a relevant drawback. An increased independence of bubbles is therefore desirable for future improvements of the introduced pump.

Package dosing with insulin shows generally slightly higher standard deviation for all package sizes (Figure 6). Similar to water dosing, the small package size of 0.05 U is challenging, since it only contains eight pump strokes. Nevertheless, four out of ten pumps

( $\mu\text{P}_3$ ,  $\mu\text{P}_5$ ,  $\mu\text{P}_6$ ,  $\mu\text{P}_9$ ) show a standard deviation under 3% and only  $\mu\text{P}_7$  and  $\mu\text{P}_{10}$  dose 0.5 mg with a standard deviation of over 10%.

### Repeatability of insulin package dosing

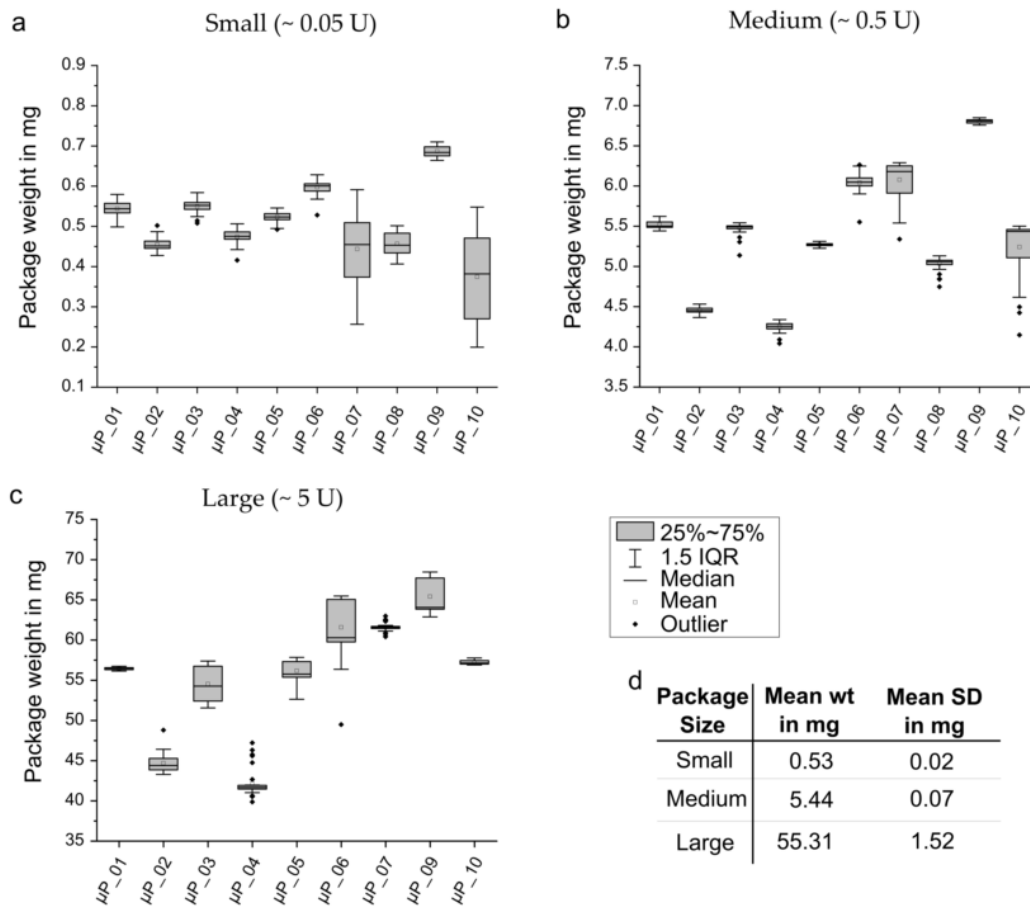


**Figure 6.** Repeatability of package dosing for each individual micropump ( $\mu\text{P}_{01}$  to  $\mu\text{P}_{10}$ ) with NovoRapid U100 insulin injection solution for small (a), medium (b) and large (c) packages of approximately 0.05 U (~0.5 mg), 0.5 U (~5 mg) and 5 U (~50 mg), respectively. The mean dosed weight and the mean standard deviation (d) are similar to experiments conducted with water.

For 0.5 U and 5 U packages, the standard deviation varies between 0.3 and 6.5%, however only two pumps,  $\mu\text{P}_6$  and  $\mu\text{P}_{10}$ , show standard deviations over 5%. The slight decrease in precision for the insulin dosing compared to water dosing is probably due to poorer priming of the fluid path, e.g., fluidic connectors and filter chamber of the test housing. The sample volume was limited and less fluid could passively be pushed through the setup to flush all air from the system. Furthermore, a high surface tension causes the liquid-air interface to be more stable for the insulin solution compared to DI water. Thus, the transport of bubbles through the valves, the pump chamber or fluidic connectors requires more pressure and has an increased impact on the fluid transport. Hence, an optimization of the pump towards higher bubble tolerance and bubble independent dosing is of even higher relevance when changing the dosed medium from DI water to insulin solution.

Overall, the experiments show a high dosing precision of the  $5 \times 5 \text{ mm}^2$  silicon pump. For 0.5 U and 5 U, only one pump shows a higher standard deviation than the generally required 5%. This high achieved precision stands out in comparison to insulin delivery units on the market. For example, Laubner et al. [10] analyze two commercially available units and show that only 20% of 0.5 U bolus are delivered within  $\pm 5\%$  accuracy [10]. The

high precision possible with this piezoelectric micro diaphragm pump for 0.5 U (5 mg packages) can therefore enable a dosing unit with higher precision than current insulin delivery systems available on the market.

The smallest package size tested in this work is not commonly tested for insulin dosing systems and most studies start their experiments with 0.5 U or 1 U [10,24]. Only Zisser et al. [25] consider small bolus sizes of 0.05 U, however, for accurate measurements, they calculate the accuracy from series of ten to twenty doses. The detection of outliers is, therefore, not possible.

The analysis of 0.05 U packages shows that most of the tested pumps are able to dose these small units precisely with seven out of ten pumps showing a standard deviation of 1.9 to 3.5%. Only two pumps dose packages with a standard deviation of more than 10%. For those pumps, a time dependent decrease in package size is visible. However, this decrease in performance is not permanent, since the pump regains the expected package size for the consecutive measurement of 0.5 and 5 U packages. The decrease can be caused by insufficient priming: enclosed air in the outlet capillary is transported to the outlet reservoir on the balance and impairs the correct detection of transported volume. Additionally, the introduced silicon pumps are bubble tolerant due to their compression ratio. However, dosing is influenced by air bubbles passing through the pump chamber. That means that the pump is able to transport the liquid–air interfaces, but the dosed package volume decreases until the chamber is filled with liquid. To achieve high accuracy even with bubbles in the system therefore requires active control. Closed-loop control systems can detect undelivered strokes and trigger compensating strokes.

The high dosing precision that we achieve with the presented pump makes a combination with higher concentrated insulin imaginable. We were able to show a similar dosing precision for 0.05 U packages that pumps on the market have for 0.5 U. Thus, it is imaginable to deliver U 500 or U 1000 insulin. The comparatively high pump chamber of the micropump enables transport of more viscous solutions due to higher insulin concentration, which will be evaluated in subsequent studies. The combination of high concentrated insulin solution with this small MEMS pump allows the development of an extremely compact and energy efficient dosing unit with only a small insulin reservoir.

#### 4. Conclusions

In the presented preliminary experiments, the introduced piezoelectric micro diaphragm pump proves well adapted for drug delivery applications. Its relatively large compression ratio (compared to other state of the art MEMS pumps) enables self-priming as well as the transport of bubbles, though the dosing precision is not independent of bubbles. The fluidic performance meets the requirements of microfluidic drug delivery. The water flow rate of  $74 \mu\text{L}/\text{min} \pm 6 \mu\text{L}/\text{min}$  allows the delivery of 10 U of insulin (0.1 mL drug solution) within 45 s, which is in the same range as macroscopic automated dosing units on the market [24]. The blocking pressure of 51 kPa of the pumps is high enough to overcome the physiological backpressure as well as additional flow restrictions due to clogging of the injection site.

The pumps show a high repeatability of package dosing. However, the precision decreases slightly with insulin compared to the transport of DI water. The higher surface tension of insulin solution increases the pressure necessary to transport air bubbles through the chamber. The decrease of precision shows that a pump that doses more independently from bubbles is desirable for the transport of insulin solution. Such a fluidic actuator can be achieved with design modifications towards a further decrease of the valve's capillary pressure and a higher compression ratio. The increased compression ratio requires a smaller pump chamber to decrease the dead volume. In future design adaptations, the compatibility of such a pump with higher concentrated drugs, and therefore, liquids with a higher viscosity, needs to be evaluated carefully. In subsequent development steps, the integration of our pump with a miniaturized, capacitive volume control will enable closed-loop control of the dosing unit, which allows for higher dosing accuracy even with

occurring disturbances. Nevertheless, the presented experimental results already show that even small packages of approximately 0.5 mg are dosed as precise as commercial pumps dose larger packages of 5 mg. Hence, the  $5 \times 5 \text{ mm}^2$  silicon micropump is suitable for a precise dosing of a U100 insulin. Furthermore, this high precision enables a combination with higher concentrated drugs, which limits the needed reservoir size as well as reduces the volume to be dosed. This enables a lower energy consumption and therefore smaller batteries. Hence, the overall size of the delivery device can be significantly reduced. The development of small and comfortable patch pumps or even implantable systems is therefore attainable.

**Author Contributions:** Conceptualization, A.B., J.H., H.L. and M.R.; methodology, A.B. and M.W.; software, M.W. and D.Z.; validation, A.B., M.W. and D.Z.; formal analysis, A.B., H.L., M.W. and D.Z.; investigation, A.B., Y.C. and D.Z.; resources, A.B., Y.C., H.L., M.R. and M.W.; data curation, M.W. and D.Z.; writing—original draft preparation, A.B., H.L. and D.Z.; writing—review and editing, A.B., J.H., M.R., H.L., M.W. and D.Z.; visualization, A.B., M.W. and D.Z.; supervision, J.H. and M.R.; project administration, A.B. and H.L.; funding acquisition, A.B., H.L. and M.R. All authors have read and agreed to the published version of the manuscript.

**Funding:** This research is part of the Moore4Medical project, which has received funding within the Electronic Components and Systems for European Leadership Joint Undertaking (ECSEL JU) in collaboration with the European Union’s H2020 Framework Program (H2020/2014-2020) and National Authorities, under Grant Agreement H2020-ECSEL-2019-IA-876190 [www.moore4medical.eu](http://www.moore4medical.eu) (accessed on 27 August 2021).

**Institutional Review Board Statement:** Not applicable.

**Informed Consent Statement:** Not applicable.

**Data Availability Statement:** The actuator stroke and fluidic test data that support the findings of this study are available in Fordatis—Research Data Repository of Fraunhofer-Gesellschaft with the identifier <http://dx.doi.org/10.24406/fordatis/143> (accessed on 27 August 2021).

**Acknowledgments:** Many thanks to Werner Regittnig for his support during the study as well as the provision of the NovoRapid samples. We thank Axel Wille for his efforts during the funding acquisition.

**Conflicts of Interest:** The authors declare no conflict of interest. The funders had no role in the design of the study; in the collection, analyses, or interpretation of data; in the writing of the manuscript, or in the decision to publish the results.

## Appendix A

**Table A1.** Overview of the material necessary for the manufacturing of the silicon micropump.

Item	Description
Monocrystalline silicon wafers (n-doped,100)	Base material for manufacturing the silicon micropump consisting (two valve wafers and one actuator wafer)
Piezoelectric disc	PIC 252; base material forming the bending actuator together with the actuator wafer
2k-epoxy glue	EPOTEK 353 ND-T, to attach the disc actuator to the pump body
O-ring	FKM material that seals the fluidic periphery with the micropump housing
Soft sealing	Costume made FKM sealing prevent leakage between the silicon micropump and the housing
Micropump housing	Special developed PEEK assembly to house the silicon micropump
Filter frit	Stainless steel filter at the inlet of the micropump housing, blocking particles larger than $5 \mu\text{m}$
Capillaries	PEEK capillaries with 1 mm inner diameter
M1 screw	Standard screw to clamp the silicon micropump to the housing with its cover

## References

1. The Diabetes Control and Complications Trial Research Group. Hypoglycemia in the diabetes control and complications trial. *Diabetes* **1997**, *46*, 271–286. [[CrossRef](#)]
2. Zisser, H.; Jovanovic, L. OmniPod Insulin Management System: Patient perceptions, preference, and glycemic control. *Diabetes Care* **2006**, *29*, 2175. [[CrossRef](#)] [[PubMed](#)]
3. Doyle, E.A.; Weinzimer, S.A.; Steffen, A.T.; Ahern, J.A.H.; Vincent, M.; Tamborlane, W.V. A randomized, prospective trial comparing the efficacy of continuous subcutaneous insulin infusion with multiple daily injections using insulin glargine. *Diabetes Care* **2004**, *27*, 1554–1558. [[CrossRef](#)] [[PubMed](#)]
4. Jeitler, K.; Horvath, K.; Berghold, A.; Gratzer, T.W.; Neeser, K.; Pieber, T.R.; Siebenhofer, A. Continuous subcutaneous insulin infusion versus multiple daily insulin injections in patients with diabetes mellitus: Systematic review and meta-analysis. *Diabetologia* **2008**, *51*, 941–951. [[CrossRef](#)]
5. Anhalt, H.; Bohannon, N.J.V. Insulin patch pumps: Their development and future in closed-loop systems. *Diabetes Technol. Ther.* **2010**, *12*, S51–S58. [[CrossRef](#)] [[PubMed](#)]
6. Zisser, H.C. The OmniPod Insulin Management System: The latest innovation in insulin pump therapy. *Diabetes Ther.* **2010**, *1*, 10–24. [[CrossRef](#)]
7. Youan, B.-B.C. Chronopharmaceutics: Gimmick or clinically relevant approach to drug delivery? *J. Control. Release* **2004**, *98*, 337–353. [[CrossRef](#)] [[PubMed](#)]
8. Lévi, F.; Focan, C.; Karaboué, A.; De La Valette, V.; Focan-Henrard, D.; Baron, B.; Kreutz, F.; Giacchetti, S. Implications of circadian clocks for the rhythmic delivery of cancer therapeutics. *Adv. Drug Deliv. Rev.* **2007**, *59*, 1015–1035. [[CrossRef](#)]
9. Bußmann, A.B.; Grünerbel, L.M.; Durasiewicz, C.P.; Thalhofer, T.A.; Wille, A.; Richter, M. Microdosing for drug delivery application—A review. *Sens. Actuators A: Phys.* **2021**, *330*, 112820. [[CrossRef](#)]
10. Laubner, K.; Singler, E.; Straetener, J.; Siegmund, T.; Päch, G.; Seufert, J. Comparative dose accuracy of durable and patch insulin pumps under laboratory conditions. *Diabetes Technol. Ther.* **2019**, *21*, 371–378. [[CrossRef](#)]
11. Bowen, J.L.; Allender, C.J. A comparative pulse accuracy study of two commercially available patch insulin infusion pumps. *Eur. Endocrinol.* **2016**, *12*, 79–84. [[CrossRef](#)] [[PubMed](#)]
12. Jahn, L.G.; Capurro, J.J.; Levy, B.L. Comparative dose accuracy of durable and patch insulin infusion pumps. *J. Diabetes Sci. Technol.* **2013**, *7*, 1011–1020. [[CrossRef](#)]
13. Borot, S.; Franc, S.; Cristante, J.; Penfornis, A.; Benhamou, P.-Y.; Guerci, B.; Hanaire, H.; Renard, E.; Reznik, Y.; Simon, C.; et al. Accuracy of a new patch pump based on a microelectromechanical system (MEMS) compared to other commercially available insulin pumps: Results of the first in vitro and in vivo studies. *J. Diabetes Sci. Technol.* **2014**, *8*, 1133–1141. [[CrossRef](#)]
14. Richter, M.; Linnemann, R.; Woias, P. Robust design of gas and liquid micropumps. *Sens. Actuators A Phys.* **1998**, *68*, 480–486. [[CrossRef](#)]
15. Kim, L.; Toh, Y.-C.; Voldman, J.; Yu, H. A practical guide to microfluidic perfusion culture of adherent mammalian cells. *Lab. Chip* **2007**, *7*, 681–694. [[CrossRef](#)]
16. Chappell, M.A.; Payne, S.J. A physiological model of the release of gas bubbles from crevices under decompression. *Respir. Physiol. Neurobiol.* **2006**, *153*, 166–180. [[CrossRef](#)]
17. Wang, Y.; Lee, D.; Zhang, L.; Jeon, H.; Mendoza-Elias, J.E.; Harvat, T.A.; Hassan, S.Z.; Zhou, A.; Eddington, D.T.; Oberholzer, J. Systematic prevention of bubble formation and accumulation for long-term culture of pancreatic islet cells in microfluidic device. *Biomed. Microdevices* **2012**, *14*, 419–426. [[CrossRef](#)]
18. Maillefer, D.; Gamper, S.; Frehner, B.; Balmer, P.; van Lintel, H.; Renaud, P. A high-performance silicon micropump for disposable drug delivery systems. Technical Digest; MEMS 2001. In Proceedings of the 14th IEEE International Conference on Micro Electro Mechanical Systems (Cat. No. 01CH37090), Interlaken, Switzerland, 25 January 2001; IEEE: Piscataway, NJ, USA, 2002; pp. 413–417.
19. Maillefer, D.; van Lintel, H.; Rey-Mermet, G.; Hirschi, R. A high-performance silicon micropump for an implantable drug delivery system. In Proceedings of the Technical Digest, IEEE International MEMS 99 Conference, Twelfth IEEE International Conference on Micro Electro Mechanical Systems (Cat. No. 99CH36291), Orlando, FL, USA, 21 January 1999; IEEE: Piscataway, NJ, USA, 2002; pp. 541–546. [[CrossRef](#)]
20. Schneeberger, N.; Blondel, A.; Boutaud, B.; Chappel, E.; Maillefer, D.; Schneider, V. Disposable insulin pump—a medical case study. In Proceedings of the DTIP of MEMS & MOEMS, Montreux, Switzerland, 12–14 May 2004; pp. 25–27.
21. International Electrotechnical Commission. *Medical Electrical Equipment—Part 2–24: Particular Requirements for Basic Safety and Essential Performance of Infusion Pumps and Controllers*; IEC 60601-2-24:2012; IEC: Geneva, Switzerland, 2016.
22. Pleus, S.; Kamecke, U.; Waldenmaier, D.; Freckmann, G. Reporting insulin pump accuracy: Trumpet curves according to IEC 60601-2-24 and beyond. *J. Diabetes Sci. Technol.* **2019**, *13*, 592–596. [[CrossRef](#)]
23. Kamecke, U.; Waldenmaier, D.; Haug, C.; Ziegler, R.; Freckmann, G. Establishing methods to determine clinically relevant Bolus and Basal rate delivery accuracy of insulin pumps. *J. Diabetes Sci. Technol.* **2019**, *13*, 60–67. [[CrossRef](#)]
24. Freckmann, G.; Kamecke, U.; Waldenmaier, D.; Haug, C.; Ziegler, R. Accuracy of Bolus and Basal rate delivery of different insulin pump systems. *Diabetes Technol. Ther.* **2019**, *21*, 201–208. [[CrossRef](#)]

25. Zisser, H.; Breton, M.; Dassau, E.; Markova, K.; Bevier, W.; Seborg, D.; Kovatchev, B. Novel methodology to determine the accuracy of the OmniPod insulin pump: A key component of the artificial pancreas system. *J. Diabetes Sci. Technol.* **2011**, *5*, 1509–1518. [[CrossRef](#)] [[PubMed](#)]
26. Wackerle, M.; Richter, M.; Woias, P.; Goldschmidtböing, F. Sub-nl flow measurement method for microfluidic actuators. In *Actuator 2000, Proceedings of the 7th International Conference on New Actuators and International Exhibition on Smart Actuators and Drive Systems, Bremen, Germany, 19–21 June 2000*; Borgmann, H., Ed.; Messe Bremen GmbH: Bremen, Germany, 2000; pp. 507–510.
27. Leistner, H.; Wackerle, M.; Congar, Y.; Anheuer, D.; Roehl, S.; Richter, M. Robust Silicon Micropump of Chip Size  $5 \times 5 \times 0.6 \text{ mm}^3$  with 4 mL/min Air and 0.5 mL/min Water Flow Rate for Medical and Consumer Applications. In *Actuator 2021, Proceedings of the International Conference and Exhibition on New Actuator Systems and Applications (GMM Conference), Online, 17–19 February 2021*; Schlaak, H., Ed.; VDE Verlag GmbH: Berlin, Offenbach, 2021; pp. 113–116, ISBN 978-3-8007-5454-0.
28. Herz, M.; Richter, M.; Wackerle, M. Method for Manufacturing a Bending Transducer, a Micro Pump and a Micro Valve, Micro Pump and Micro Valve. Patent No. US9410641B2, 9 August 2016.
29. Richter, M.; Wackerle, M.; Congar, Y.; Drost, A.; Häfner, J.; Röhl, S.; Kibler, S.; Kruckow, J.; Kutter, C. Miniaturisierung von Mikromembranpumpen für die Integration in Mobilfunkgeräte. In *MicroSystemTechnik Kongress 2017, Proceedings of MST 2017, München, Germany, 23–25 October 2017*; VDE Verlag GmbH: Berlin, Germany, 2017.
30. Woias, P. Micropumps—Past, progress and future prospects. *Sens. Actuators B Chem.* **2005**, *105*, 28–38. [[CrossRef](#)]